

Thermodynamic Properties of Nonideal Gases.

I. Free-Energy Minimization Method*

H. C. Graboske, Jr., D. J. Harwood, and F. J. Rogers

Lawrence Radiation Laboratory, University of California, Livermore, California 94550

(Received 9 May 1969)

The thermodynamic properties of nonideal or interacting gases are studied using a thermodynamically consistent method which derives a state function for the gas from a separable Hamiltonian for the many-body system. The state function – the Helmholtz free energy – is a sum of translational, configurational, and internal components, and the statistical equilibrium state is calculated on a computer by minimizing the free energy in composition space at a given volume and temperature. A series of free-energy models is constructed to investigate the effects of various interactions. The effects on the equilibrium state of including Fermi-Dirac statistics in the translational free energy is shown to be small, while Coulomb and excluded-volume configurational terms produce large thermodynamic effects. The most important interaction effect, the modification of the internal partition function, is studied using a free-atom model and a confined-atom model which introduces volume- and temperature-dependent energy eigenvalues and partition-function sum terminations. The free-energy minimization method is shown to be a versatile and efficient tool for studying interacting gases, and provides quantitative estimates of the limits of validity of the various interaction models.

1. INTRODUCTION

This paper presents the initial results of a systematic study of the thermodynamic properties of nonideal multicomponent mixtures of gases. In astrophysical problems, among others, one requires the calculation of dissociation and ionization equilibria and associated thermodynamic properties, such as pressures, internal energies, and specific heats, over a very wide range of temperatures and densities for mixtures of gases containing a variety of species. A number of physical effects enter the theory of gases at various density-temperature regions, including degeneracy effects, Coulomb interactions of free charges, ionization potential lowering, pressure dissociation and ionization, excluded volume effects, and bound-state level shifts and broadening. A variety of theoretical models has been developed to describe these effects to some degree of accuracy in various (ρ, T) regions. The general problem is quite complex, and even single aspects such as the Coulomb interaction in a fully ionized gas have no rigorous theoretical results of general validity.

The present study extends the theoretical format and numerical procedure originated by Harris,^{1,2} which has the advantage of obtaining thermodynamic consistency by defining the many-body system in terms of a unique total partition function (or equivalent Helmholtz free energy) and determining numerically from this fundamental state function, the statistical equilibrium state and the ther-

modynamic properties. Other advantages of this free-energy minimization method are that it allows treatment of all nonideal effects simultaneously and readily incorporates systematic theoretical improvements of a specific nonideal term. It handles arbitrarily complex chemical mixtures, and by monitoring various interaction parameters, can determine the limits of validity of the various approximate nonideal models being used in the calculation.

In the following sections, we first define the thermodynamic formalism and numerical methods, and then proceed to analyze various free-energy models. The effect of incorporating Fermi-Dirac statistics is presented, then a detailed comparison is made of the internal partition function for free and confined atoms. Two configurational terms are studied; the Coulomb interaction in a simple form, and a high-order theory for the excluded volume effect of a hard-sphere mixture.

2. THERMODYNAMIC FORMALISM AND NUMERICAL METHOD

For a physical system of specified particle numbers $\{N_i\}$, volume V , and temperature T , an appropriate description of the statistical ensemble is given by the canonical partition function Z_C or by its associated thermodynamic potential, the Helmholtz free energy F . The partition function is defined in terms of a phase integral containing a many-body Hamiltonian of the form

$$\mathcal{K}(\vec{p}_1, \vec{p}_2, \dots, \vec{p}_N; \vec{r}_1, \vec{r}_2, \dots, \vec{r}_N)$$

$$= \sum_{i=1}^N \frac{\vec{p}_i^2}{2m} + U(\vec{r}_i^N), \quad (2.1)$$

where $U(\vec{r}_i^N)$ is the many-body interaction potential, the momentum and potential functions being assumed to be uncoupled. This leads to a factorizable many-body partition function, having translational, configurational, and internal factors,

$$Z_c = \left[\frac{1}{h^{3N}} \int \dots \int \exp \left(-\beta \sum_{i=1}^N \frac{\vec{p}_i^2}{2m} \right) \prod_{i=1}^N d\vec{p}_i \right]$$

$$\times \left[\frac{1}{N!} \int \dots \int \exp[-\beta U(\vec{r}_1, \vec{r}_2, \dots, \vec{r}_N)] \prod_{i=1}^N d\vec{r}_i \right]$$

$$\times \left[\sum_{j=1}^{\infty} g_j \exp(-\beta E_j) \right] = Z_{\text{trans}} Z_{\text{config}} Z_{\text{int}}, \quad (2.2)$$

where $\beta \equiv kT^{-1}$.

The translational term reduces to a product of N one-body terms, and it is possible to reduce the intractability of the general configurational term by making certain assumptions, for example, that $U \equiv 0$ (the ideal gas), or that

$$U(\vec{r}_1, \vec{r}_2, \dots, \vec{r}_N) = \sum_{i < j} u(\vec{r}_i, \vec{r}_j).$$

Here an N -body interaction potential is replaced by a sum of $\frac{1}{2}N(N-1)$ pair potentials. This configurational potential will be called an external potential to emphasize its interparticle nature.

The internal partition function includes the sum over all bound levels, whose energy eigenvalues are determined by solving a Schrödinger's equation for each bound system. The internal Hamiltonian also has a potential term $\mathfrak{u}(\vec{r}_1, \dots, \vec{r}_N, \vec{p}_1, \dots, \vec{p}_N)$ which is represented by the Coulomb potential of the nucleus (independent of \vec{r}_i, \vec{p}_i), as modified by perturbations (functions of \vec{r}_i, \vec{p}_i). In general, the internal potential $\mathfrak{u}(\vec{r}_i, \vec{p}_i)$ should represent an atomic system whose properties are consistent with the interparticle potential $U(\vec{r}_i, \vec{p}_i)$ that describes the interaction between other particles and the bound system. An example of a consistent set of internal potentials in the ideal gas, where the external potential is assumed to be zero and the internal potential is the unperturbed Coulomb potential of the nucleus (the free or isolated atom model). Another example is the Coulomb gas, the external potential being the screened Coulomb potential between charged particles, and

the internal potential given by a screened nuclear Coulomb potential.

Once the state function of the system has been specified, all the thermodynamic properties of the gas are immediately derivable. If the total partition function of the system is factorizable, as in (2.2), then the free energy may be written as the sum of three types of terms:

$$F = F_{\text{trans}} + F_{\text{config}} + F_{\text{int}} = F(\{N_i\}, V, T). \quad (2.3)$$

The condition of thermodynamic equilibrium requires that for a system at specified volume V and temperature T ; the free energy must be a minimum. The equilibrium state is determined by minimizing the free energy with respect to the particle numbers $\{N_i\}$, subject to the stoichiometric constraints. If F is expressible as an analytic differentiable form, these equations can be solved by differentiating F with respect to $\{N_i\}$ and forming a set of simultaneous nonlinear equations in $\{N_i\}$, V , and T , the equilibrium composition equations. This set is generally solved iteratively for the equilibrium values of $\{N_i\}$, and the thermodynamic properties then are evaluated. The following schematic representation defines the quantities of interest and summarizes the procedure:

(i) Definition of model:

$$F = F(\{N_i\}, V, T).$$

(ii) Determination of equilibrium state by minimization of F :

$$\sum \left(\frac{\partial F}{\partial N_i} \right)_{V, T} \nu_{ij} = 0, \quad \text{for all } j$$

$$\Rightarrow F = F_{\text{equil}}(\{N_i\}_{\text{equil}}).$$

(iii) Calculation of thermodynamic properties:

$$P = - \left(\frac{\partial F_{\text{equil}}}{\partial V} \right)_{\{N_i\}_{\text{equil}}}, T,$$

$$S = - \left(\frac{\partial F_{\text{equil}}}{\partial T} \right)_{\{N_i\}_{\text{equil}}}, V,$$

where ν_{ij} is the stoichiometric matrix, and P and S are pressure and entropy. The particle number is replaced in the calculations by $X_i = N_i/N_0$ (N_0 is Avogadro's number), which is the number of particles per initial particle or the mole number.

In practice, this scheme is not trivial even for the simplest real systems such as the ideal (non-interacting) classical gas. This system results in a set of nonlinear equilibrium equations, the Saha equations, which must be solved iteratively. In addition, the internal free energy is generally approximated as a ground-state term only, with temperature-dependent corrections to account for excited-state contributions. Introducing various nonideal terms into the state function, F greatly increases the difficulty of obtaining approximate analytic solutions.

Using the free energy to specify the many-body system and to derive the full thermodynamic description of the gas has several advantages. First, the method is thermodynamically consistent, and by definition satisfies all the thermodynamic relations. It admits of a modular approach, allowing successive models of many-body systems to be introduced and evaluated by a standard procedure. The method contains internal checks for validity of the various models, and by calculating interaction parameters which characterize various non-ideal effects, we can delineate regions of validity for the various models.

The method used to find the minimum of the free energy of the system by means of a digital computer is similar to that described by Harris.^{1,2} The various contributions to the free energy are obtained through a series of subroutine calls. Analytic expressions are used where they exist, otherwise high-accuracy (6–8 place) fits are made to numerical evaluations of complicated integrals. The complexity of the internal partition function leads to a relatively long computation time; therefore, a table is generated from which intermediate values are obtained by a bivariate La Grange interpolation. The procedure is to start with an arbitrary choice of the equilibrium composition $\{N_i\}$ at a given (V, T) and to make a series of small changes in the composition through the stoichiometric equations. The size and direction of the shift that is made with a particular equation is determined by the free-energy change with respect to the previous cycle. The procedure is similar to the method of steepest descents. Two criteria are used to determine when equilibrium has been reached. First, all possible changes in the partial molar concentrations of magnitude $\Delta x \approx 10^{-4}$ increase the free energy. Second, an independent initial composition is chosen and the system is required to return to the same equilibrium composition to within Δx_i (usually 10^{-4}).

After the equilibrium composition is obtained, the equation of state and thermal properties are calculated by evaluating the appropriate partial derivatives of the free energy.

3. EFFECTS OF FERMI-DIRAC STATISTICS

If interactions between gas particles are assumed negligible, the Helmholtz free energy of

an ideal classical gas at temperature T and volume V is given by

$$F = kT \sum_i \left\{ \ln \left[\frac{N_i}{g_i V} \left(\frac{h^2}{2\pi m k T} \right)^{3/2} \right] + 1 \right\} - kT \sum_i N_i Z_i(T) - \frac{4\sigma}{3c} VT^4, \quad (3.1)$$

where N_i is the number of particles of type i , m_i is the mass, g_i is the spin statistical weight, $Z_i(T)$ is the internal partition function, σ is the Stefan-Boltzmann constant, and c is the velocity of light. The first term in (3.1) is the free energy of a noninteracting gas of point particles F_1 . The next term F_2 , is the free energy due to internal structure (to be discussed in Sec. 4) and the last term F_3 , is the free energy due to the photon gas, which is important at high temperatures.

At low temperatures or high densities, the effects of Fermi statistics become important, yet it has long been known³ that inclusion of Fermi-Dirac (FD) statistics at high densities fails to remove the shift to neutrality of the classical equilibrium equations. To see the effect of treating the fermions rigorously (considering regions where only electrons need to be treated by quantum statistics), the free energy of the electrons, rather than being represented by a term of the form of F_1 , will be given by

$$F_3 = kTN_e \{ \alpha_e - [\mathfrak{F}_{3/2}(\alpha_e)/\mathfrak{F}_{1/2}(\alpha_e)] \}, \quad (3.2)$$

$$\text{where } \mathfrak{F}_p(\alpha) \equiv \frac{1}{\Gamma(p+1)} \int_0^\infty \frac{t^p dt}{e^{t-\alpha} + 1}. \quad (3.3)$$

The parameter α_i which characterizes the degeneracy is the chemical potential divided by kT for the species i and is determined through the relation

$$\mathfrak{F}_{1/2}(\alpha_i) = \frac{N_i}{g_i V} \left(\frac{h^2}{2\pi m k T} \right)^{3/2} \equiv f. \quad (3.4)$$

In the classical limit ($f \rightarrow 0$ or $\alpha \ll -1$), the expression for F_3 reduces to the same form as F_1 . However, F_3 increases more rapidly than F_1 as a function of f (both are monotonic increasing functions of f) and the difference between the two becomes quite noticeable for $f > 1$ ($\alpha > 0$). The effect of the Fermi-Dirac statistics is therefore to increase the free energy for a given composition V and T above what it would be in the case of classical statistics. The composition shifts to minimize the free energy at equilibrium, and since F_3 is monotonic increasing in N_e , the equi-

librium shifts in the direction of smaller N_e or, in other words, toward neutralization. A decrease in the volume increases f and causes a shift toward equilibrium in the case of either classical or quantum statistics, but the effect is more pronounced in the quantum case. This suppression of ionization due to degeneracy of the free electrons is expected because of the reduced volume in phase space available to free electrons caused by operation of the exclusion principle.

By minimizing the free energy of the system, a set of coupled equilibrium concentration equations can be derived for the system. The result is a Fermi-modified Saha equation for the i th stage of ionization,

$$\frac{N_{i+1}}{N_i} N_e = \frac{Z_i(T)}{Z_{i+1}(T)} N_e^{-\alpha_e} \quad (3.5)$$

In the classical limit ($\alpha_e \ll -1$), using (3.4) and the asymptotic approximation

$$N_e^{-\alpha_e} \approx [\mathfrak{F}_{1/2}(\alpha_e)], \quad (3.6)$$

Equation (3.5) reduces to the standard Saha equation.

The addition of degeneracy to the classical equilibrium equation is seen to have two features: It predicts lowered ionization relative to the classical result, and it modifies the classical result by at most a few percent. At sufficiently low volume, both models predict a complete shift to neutral atoms and then to molecules. Although inclusion of Fermi statistics is critical to the accuracy of the thermodynamic properties at low volume, by itself this effect predicts an incorrect equilibrium state.

The pressure due to the electrons can be shown to be

$$P_3 = (N_e kT/V) [\mathfrak{F}_{3/2}(\alpha_e)/\mathfrak{F}_{1/2}(\alpha_e)], \quad (3.7)$$

a monotonic increasing function of N_e , which is larger than the corresponding case for classical statistics for a given N_e , V , and T . It is worthwhile to note, in practice, P_3 is very little affected by the statistics in the region where the gas is partially ionized because the effects of having less electrons but greater pressure per electron nearly compensate for each other. Where the gas is fully or nearly fully ionized, however, the statistics cause an appreciable increase in the pressure.

Using the free-energy minimization method, equilibrium calculations were performed for an ideal hydrogen gas, using both Maxwell-Boltz-

mann (MB) and FD statistics, which numerically reproduced the theoretical conclusions reviewed above. The numerical methods for computing the FD integrals involve use of highly accurate analytic fits valid for any value of α . A high degree of accuracy is necessary since the free-energy surface near the minimum typically has variations of 1 part in 10^6 , so that numerical errors in the free-energy expressions, which are greater than this, can lead to erroneous equilibrium results. For all the following free-energy models, the ideal-gas terms include MB statistics for classical particles and FD statistics for all fermions.

4. NONIDEAL ELECTRONIC EFFECTS FROM BOUND-STATE PERTURBATIONS

The calculation of equilibrium composition in a reactive system depends on the internal partition function of the ensemble of bound states. For an arbitrary mixture of molecules, molecular ions, atoms, and ions, this function is mathematically complicated and depends upon a great number of specific pieces of physical data. The eigenstates of the bound system are determined from experiment or from solution of Schrödinger's equation which contains the multiparticle internal potential $\mathfrak{U}(\vec{r}_i, \vec{p}_i)$.

A fundamental requirement for the internal model of a bound system is that the potential in the wave equation be consistent with the physical behavior of the system as described by the configuration terms. As an example, if a system of strongly ionized gas includes a Coulomb-interaction configurational free energy, it is logical to require the internal states to experience that same Coulomb potential which the free charges obey. Or, if a gas has many bound systems, whose available volume is modified by some hard-sphere approximation in the configurational free energy, it would be consistent to include an atomic system whose eigenstates correspond to a very stiff or hard core with no interpenetration of the outer orbitals of neighboring atoms. What is inconsistent is to include large configurational effects while assuming the electronic bound states are unperturbed.

Let us now describe two basic theoretical models which represent bound-state systems in a gas. These models are the isolated or free atom and the confined atom. The isolated one-electron atom is defined by a potential function

$$\mathfrak{U}(r) = -Ze^2/r, \quad 0 \leq r \leq \infty. \quad (4.1)$$

The resultant hydrogenic eigenstates have l -degenerate energy eigenvalues which are independent of the state variables V and T . These electronic energies of the isolated atom (IA) are then

used in the internal partition function for the system,

$$\left(Z_{\text{int}}^{\text{IA}}\right)_i = (2S_i + 1) \sum_{j=1}^{\infty} g_j e^{-\beta E_j} (Z_{\text{vib}} Z_{\text{rot}}), \quad (4.2)$$

where S_i is the nuclear spin of species i , g_j is the electronic-state statistical weight, and $Z_{\text{vib}} \times Z_{\text{rot}}$ represents the partition function for vibration and rotation of the molecular species. The corresponding free energy is

$$F_2^{\text{IA}} = -kT \sum_i N_i \ln \left(Z_{\text{int}}^{\text{IA}}\right)_i. \quad (4.3)$$

The termination of the free-atom electronic partition function is generally determined by either an *ad hoc* criterion resulting from some physical model, or by computational convenience. Given an internal partition function of this type, one can use the resultant isolated atom internal free energy to compute the Saha-Boltzmann equilibrium composition equations.

The central problem of thermodynamic equilibrium at high density lies in the consistent determination of the density and temperature dependence of the perturbed electronic energy levels and of the partition function cutoff. These related problems have been treated by various *ad hoc* approaches,⁴ since the exact solutions require the knowledge of the many-body interparticle potentials and the corresponding solutions to the many-body wave equation for all species of the system (both multielectron and multiatom species). Computationally, this problem exceeds current capabilities. However, it is possible to introduce an approximate atomic potential into the Hamiltonian and proceed to evaluate the equilibrium in a thermodynamically consistent manner. This removes the inaccuracies of putting *ad hoc* approximations such as energy level shifts and level cutoffs into the system without including them as an integral part of the thermodynamic-state function.

The confined atom model (CA) of a perturbed atom is more consistent with the various configurational effects discussed below than is the IA model. The confined atom potential is given by

$$\begin{aligned} \mathfrak{U}(r) &= -Ze^2/r, & 0 \leq r < r_0, \\ &= +\infty, & r \geq r_0, \end{aligned} \quad (4.4)$$

and is simply a hydrogenic atom confined in a spherical cell of radius r_0 with hard walls. This model, developed by Harris *et al.*,² approximates a one-electron atom which is confined to a spherical region of mean radius r_0 by hard-sphere interactions with neighboring bound systems, whose

outer electronic orbitals are noninterpenetrating.

The primary requirements of a perturbed atom are that the atomic properties of the system be consistent with its external characteristics (its interaction with other systems). Since this model assumes that atomic interactions appear on the average to create an effectively hard boundary through nearest-neighbor interactions, the atomic eigenstates should exhibit this hard-core behavior.

The confined hydrogenic atom Schrödinger equation⁵ has as radial eigenfunctions the confluent hypergeometric functions. The resultant energy eigenvalues are dependent on the cell radius r_0 , and the l degeneracy of the electronic levels is destroyed, highest l states lying lowest in energy. There is a minimum value of r_0 for which each n, l state changes from real eigenvalues through zero to imaginary eigenvalues, which can be interpreted as the transition from states of negative energy (bound) to states of positive energy (free) leading to a cutoff position for the two-particle bound state.

The first six energy eigenvalues for the hydrogen atom in the CA model are given in Fig. 1. The characteristics of this model are that it closely approximates the isolated atom even when r_0 is as small as a few Å. Then the energy increases very rapidly with decreasing r_0 until it reaches zero at some specific value $r_0^c(n, l)$, the cutoff radius for that level. It is apparent that this model is an extreme version of the nonideal atom, exhibiting very little perturbation until near the cutoff and then showing a rapid and large change. One would expect this to produce a much more abrupt behavior in the thermodynamic properties than a more long-range perturbation.

The internal structure of the confined atom is in fact reasonably consistent with the physical features of its external interaction. The very steep radius dependence of E_{nl} exhibited in Fig. 1 indicates that such a system would be a very hard or incompressible atom. This feature corresponds to the sharp cell boundary produced by the confining effect of the neighboring atoms, and is also consistent with a hard-sphere configurational term (an excluded volume effect), a feature later incorporated in the model.

While the confined atom internal partition function is consistent with the external potential of a hard-sphere gas, it has several deficiencies which lessen its applicability. First, it is not a close approximation to the perturbation produced by the Coulomb potential of the charged particles present in the system. This perturbation is dominant in the region of strong ionization, and is a longer-range effect⁶ with a more gradual r dependence and a much smaller range for destruction of the ground state (0.445 Å versus 0.97 Å). Further, the l inversion of the levels is the reverse of the Coulomb perturbation which produces

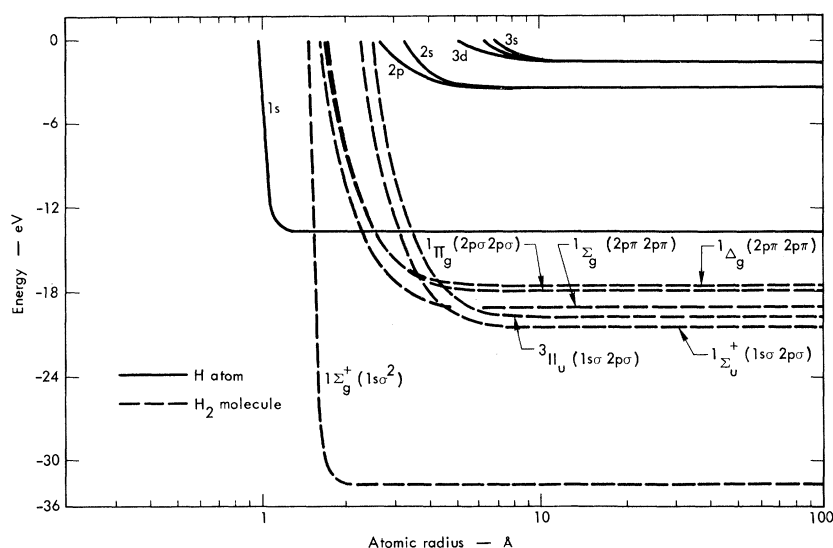


FIG. 1. Energy levels for the confined atom (CA) model of bound states of the H atom and H_2 molecule. At large values of atomic cell radius, the CA energies approach the isolated-atom (IA) values.

level separation with lowest l levels lying lowest in energy. The CA energy eigenvalues, thus, only crudely approximate the Coulomb level shifts in the atoms present in the high-temperature gas.

At low temperatures, the model is more realistic, but another problem is present. The CA potential corresponds to an unperturbed hydrogenic potential with a boundary condition that the radial eigenfunction for all levels vanish at r_0 (rather than at ∞ as in the isolated atom). In the high-density low-temperature limit, one expects to reach a metallic state where periodic boundary conditions apply, a feature not present in the current CA model. This limits the present model at high density to the high-temperature region, where a fully ionized dense plasma is the final state.

The partition function cutoff, or maximum number of bound states $n_{\max}(r_0)$, resulting from counting the number of bound states allowable in a cell of radius r_0 , is plotted for hydrogen in Fig. 2. The cutoff positions are shown for 24 states of the H atom, the l values being reversed for each energy value of n . The $1s$ state is much more stable than the next most stable state $2p$.

The CA internal partition function and free energy are given by

$$(Z_{\text{int}}^{\text{CA}})_i = (2S_i + 1) \times \sum_j^{n_{\max}(V, T)} g_j e^{-\beta E_j(V, T)} (Z_{\text{vib}} Z_{\text{rot}}), \quad (4.5)$$

$$F_2^{\text{CA}} = -kT \sum_i N_i \ln(Z_{\text{int}}^{\text{CA}})_i, \quad (4.6)$$

where $E_j(V, T)$ are the CA perturbed energy levels and $n_{\max}(V, T)$ is the maximum number of bound

states.

Since the CA exact results apply only to one-electron systems, some method must be devised to extend the model to multielectron and multi-atom (molecular) systems. This has been done in a modified version of Harris's method⁶ by replacing the actual multielectron orbitals with a set of one-electron CA orbitals. The method used by Harris normalized the energy levels only, and the resultant atomic and molecular radii for multielectron systems varied widely from measured values. For example, the H_2 molecule resulting from an energy normalization of the ground-state orbitals has a smaller cutoff radius than the H atom, with the result that pressure ionization occurred at lower densities than pressure dissociation. To eliminate this feature, the resultant combined CA orbitals are normalized to free-atom (unperturbed) values by requiring both the atomic energies and radii to be equivalent. First, the total energy of the system is equated to the measured or computed free-atom energies

$$E_i = \sum_j \frac{Z_{ij}^2}{n^2} R_0 f(V, T) \equiv E_i(\infty), \quad (4.7)$$

where the sum is over all j electrons, n is the

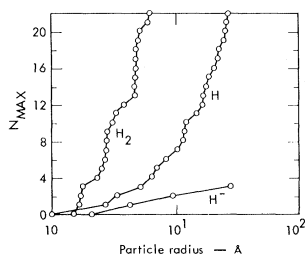


FIG. 2. Number of bound states in the CA model for H, H^+ , and H_2 , representing the cutoff of the sum over states for this form of the internal partition function.

unperturbed energy eigenvalue, R_0 is the Rydberg. Z_{ij} is the effective nuclear charge for species i and electron j , $f(V, T)$ represents the functional form of the CA energy eigenvalue dependence on V and T , and $E_i(\infty)$ is the experimental or computed energy of the isolated-atom eigenstate.

For the outer electron (i_{\max}), the ground-state orbital ($j=1$) must be normalized to the effective radius of the atom, of mass number A_i . This is done by setting

$$r_0^c(A_i) = \frac{r_0^c(H)}{Z_{i \max, j=1}} = r_{\text{expt}}(A_i), \quad (4.8)$$

where $r_0^c(H)$ is the cutoff radius for the n, l level in the H atom. The actual radius is obtained from experimental values, or from the actual electronic charge-density distributions computed for the free atom of type A_i , in the HFS method.⁷ By thus normalizing the multielectron CA atomic orbitals, the resultant CA model has exactly the isolated-atom energies and radii for large r_0 . The results of this procedure are shown in Figs. 1 and 2. In Fig. 1, the energy levels of the CA model of H_2 are shown, having the same qualitative behavior as the H eigenvalues, and reproducing the free-molecule system at larger r_0 . In Fig. 2, the maximum number of bound states is given for H_2 and H^- in the CA model. The molecules show a much closer spacing of n_{\max} in r_0 space, where the H^- ion is closer to the H atom in its r_0 dependence. The values of r_0^c for the four-bound systems are:

Species	Ground state	$r_0^c(\text{\AA})$
H	1s	0.97
H^-	(1s) ²	2.05
H_2	1s σ , 1s σ	1.48
H_2^+	1s σ	2.12

The computational data for the internal free energy F_2 consists of the CA eigenvalues for 83 states, and for each type of particle, the charge, mass, electron number, total number of states, statistical weight, and effective nuclear charge for each state, and all necessary molecular data. The FMIN code then calculates the internal partition function for each species for a range of r_0 (10^5\AA to r_0^c) and T (0.01 – 10^4 eV) and the resultant F_2 values are tabulated. The actual calculation of the total F_2 is carried out by performing a high-order interpolation in the F_2 table for each species. The value of T is directly available, and the value of r_0 is dependent on $\{x_i\}$ and V .

The physical effect represented by the CA model is the confinement of a bound system by the presence of its neighbors, which act to confine it to an average spherical volume of radius r_0 . Each species is given that proportion of the total volume

available to the entire system which equals the ratio of its actual hard-sphere volume to the total hard-sphere volume of all bound species. Electrons and bare nuclei are assigned zero excluded volume.

$$(r_0)_i = (r_0^c)_i \left\{ V \left[\frac{4}{3} \pi N_0 \sum_i x_i (r_0^c)_i^3 \right]^{-1} \right\}^{1/3}. \quad (4.9)$$

Given the atomic radii $(r_0^c)_i$, composition set $\{x_i\}$, V , and T , one computes $(r_0)_i$ for each species and then finds the corresponding internal free energy F_2 in r_0 , T space.

In this study, the basic hydrogen-gas system contains six components: H_2 (32 states, 6 multiply excited), H_2^+ (3 states), H^- (4 states, 2 doubly-excited states theoretically predicted), H (83 states), H^+ , and e^- . Defining two total free-energy models as the isolated atom (IA) and confined atom (CA) models,

$$F^{\text{IA}} = F_1 + F_2^{\text{IA}} + F_3 + F_7, \quad (4.10)$$

$$F^{\text{CA}} = F_1 + F_2^{\text{CA}} + F_3 + F_7, \quad (4.11)$$

where F_1 is the free energy of the noninteracting Maxwellian particles [the first term in Eq. (3.1)], F_3 is the free energy of the fermions [Eq. (3.2)], F_7 is the free energy of the photon gas [third term in (3.1)], while F_2^{IA} and F_2^{CA} are internal free energies given by Eqs. (4.3) and (4.6). The equation for F^{IA} is the model of the ideal gas with FD statistics included, while F^{CA} is the model of the nonideal gas with CA bound-state perturbations.

Using the six-component hydrogen gas and the FMIN code, the resultant equilibrium compositions are shown in Fig. 3. The behavior of the two models is identical at high volume, both predicting complete dissociation and ionization at the highest V values. As V decreases, the equilibrium shifts toward large clusters, recombination at higher temperatures, and association at lower temperatures. Here, the models predict increasingly different results, the CA model giving, at first, slightly enhanced ionization above the IA results. Then, in the region 0.05 – 0.1 cm^{-3} , pressure dissociation is observed in the CA model results at 0.5 eV . From 10^{-1} cm^{-3} to very small volumes, progressively complete pressure ionization occurs in the CA model at all temperatures. Conversely, the IA model predicts at high density, complete recombination and, at low temperatures, complete association. The significance of this comparison is that a thermodynamically consistent equilibrium state can be produced using the CA model to represent the bound-state perturbation. No configurational nonideal terms can do this in a consistent manner, and in fact none are

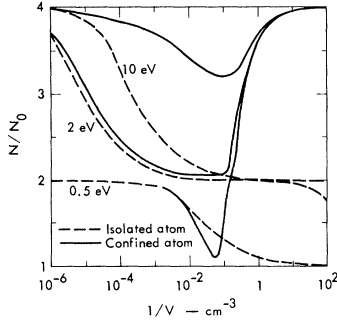


FIG. 3. Equilibrium composition for hydrogen as a function of V^{-1} . This variable is chosen because it contains the value of the independent-state variable V , while being proportional to the physical variable ρ , mass density ($V^{-1} = \rho/m_0$, where m_0 is the mass of the initial composition of 1 mole of H_2 , 2.01 g). The equilibrium composition is defined here as total particle number divided by Avogadro's number, which also is the total mole number $N/N_0 = x_t$. The two free-energy models illustrated here include the internal partition function for the isolated and the confined atom.

needed to achieve the correct composition in the high-density limit. The equilibrium composition results of the CA model are not exact due to omission of the configurational terms, but they do represent a qualitatively correct picture of bound-state perturbations by neighboring bound systems in the high-temperature and high-density limit.

The resultant pressure equation of state is illustrated in Fig. 4. The partial pressures (defined here as the negative volume derivative of the various F terms) produced with the IA model are everywhere the perfect gas pressure (not plotted). Since it predicts recombination before electron degeneracy becomes significant, the inclusion of FD effects in F_3 has a negligible effect on the thermodynamic properties.

The partial pressures computed with the CA model show a variety of effects. At low densities, the pressures are nearly equal to the perfect gas pressures, but as the region of nonideal effects is reached, the contribution from the translational terms rises due to pressure dissociation and ionization. The electron pressure rises sharply as the bound electrons are freed at volumes where they are moderately degenerate at the start. The electrons rapidly become strongly degenerate, providing the largest pressure contribution at high densities.

A completely new, nonideal pressure term appears, given by

$$P_2 = - \left(\frac{\partial F_2}{\partial V} \right) \{N_i\}, T,$$

which represents the pressure arising from the volume dependence of the internal partition function. In the CA model, this nonideal contribution is the dominant term in the volume region 10^{-1} – 0.5 cm^{-3} . The bound-state pressure effect is so large here because of the sharp behavior of the internal perturbation, having a very strong volume dependence near the cutoff radius of the atomic cell. This is seen in the energy-level diagram (Fig. 1), where the energy climbs very rapidly in the region $2r_0 - r_0$. Since at low temperature, F_2 is strongly dependent on $E_{1s}(r_0)$ and r_0 is proportional to $V^{1/3}$, we can relate $\partial F_2 / \partial V$ to $\partial E_{1s} / \partial r_0$ and see that one indeed would expect a large contribution to the pressure to arise from F_2 in the dissociation and ionization zone. The important point here is that a thermodynamically consistent theory of ionization must have just such a term in the equations of state. A strong perturbation of the bound states must be consistently reproduced not only through the pressure effects resulting from increase in equilibrium particle number (seen in P_1 and P_3) but also from the volume and temperature dependence of the internal partition function.

Although the CA model used here represents a simple and extreme approximation to the real interparticle bound-state perturbation in a charged dense gas, it demonstrates that this factor can by itself produce high-density ionization. In the following sections, it is demonstrated that configurational perturbations, although important, cannot produce a consistent physical model of this criti-

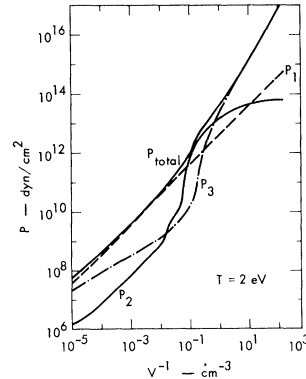


FIG. 4. Equilibrium pressure for hydrogen at 2 eV. The classical ion pressure P_1 is almost linear. The electron pressure P_3 demonstrates classical recombination effects at low density, pressure ionization at intermediate density, and strong degeneracy at high density. The pressure due to volume dependence of the internal partition function P_2 reaches large values during the ionization process, contributing significantly to the total pressure over the region $10^{-1} \text{ (cm}^{-3}) \leq V^{-1} \leq 10^1 \text{ (cm}^{-3})$.

cal effect. For the remainder of this paper, the base model used for comparison will be the CA model as given in (4.11).

5. NONIDEAL CONFIGURATION EFFECTS FROM COULOMB INTERACTION

In a strongly ionized gas, the major nonideal effect is known to be the Coulombic interactions between the charged components. This Coulomb perturbation enters the partition function in two ways. Through the interparticle interaction potential it modifies the configuration integral, and through the internal potential, it perturbs the bound states. The latter effect should properly be discussed in connection with the internal partition function, and these bound-state Coulombic effects will be discussed in detail in a later paper.

The most fundamental and rigorous approach to the treatment of systems of charged particles interacting via Coulomb forces is the use of perturbation methods of quantum field theory with diagrammatic expansions of the grand partition function of the interacting many-body system.⁸ This mathematically complex procedure leads to difficult integrals, whose solution removes the long-range divergence of the Coulomb potential by summing chains of Coulomb interactions to obtain the Debye (static) screened potential. The short-range divergence is removed by summing a two-particle series in (e^2/r) to give a short-range cutoff arising from the uncertainty principle. A subsequent paper contains a detailed application of the quantum cluster theory in the configurational free energy.

Because of the great complexity of this configurational term, we use here a slight modification of the simple Debye-Hückel (DH) model adopted by Harris *et al.*² This first approximation is rigorously valid only in the high-temperature low-density limit, but it does provide an estimate of the size and significance of the effect.

The Helmholtz free energy of this model is given by

$$F_4 = -kT \sum_i N_i \left(\frac{\Lambda_F}{3} \right) \tau \left(\frac{r_{\min}}{\lambda_F} \right). \quad (5.1)$$

The plasma interaction parameter Λ_F is

$$\Lambda_F = 2\pi^{1/2} e^3 \left(\sum_i z_i^2 N_i \theta_i / V \right)^{1/2} \beta^{-3/2}, \quad (5.2)$$

and the generalized multicomponent screening length is

$$\lambda_F = [4\pi\beta e^2 \sum_i z_i^2 (N_i \theta_i / V)]^{-1/2}, \quad (5.3)$$

$$\theta_i = \mathcal{F}_{-1/2}(\alpha_i) / \mathcal{F}_{1/2}(\alpha_i). \quad (5.4)$$

The sum is carried out over all charged species. This definition of screening takes into account the screening by all types of charged species, and includes the FD statistics. The term λ_F is identical to the classical Debye length in the low-density region, where $\theta_i = 1$; otherwise, the screening length is somewhat larger since $\theta_e \rightarrow 0$ in the case of extreme degeneracy of the electrons. The short-range divergence of the DH model can be eliminated by the rigorous quantum-mechanical cluster expansion method.⁹ This is a complex mathematical formalism currently being adapted for direct application to a general system of arbitrary V and T . To eliminate the short-range divergence, we adopt the approach where a modified solution theory cutoff is used. The function

$$\tau(x) = 3 [\ln(1+x) - x + \frac{1}{2}x^2] x^{-3} \quad (5.5)$$

(with $x = r_{\min}/\lambda_F$) as a multiplier in (5.1) may be shown¹⁰ to provide such a cutoff. We define the distance of closest approach as

$$r_{\min} = \langle z \rangle e^2 / E_F, \quad (5.6)$$

where $\langle z \rangle$ is the average charge of the positive ions, and E_F is the average energy of the free electrons (fermions). In the limit that $r_{\min} \rightarrow 0$, $\tau \rightarrow 1$; otherwise, $\tau < 1$.

Consider the effect of this interaction term in an even simpler case, where we assume $\tau = 1$ and $\theta_i = 1$. In this case, when the free energy from (5.1) is included in the total free energy for an isolated-atom model, a modified Saha equation describing the system can be derived in which the only modification is that the ionization potential E_0 is replaced by $E_0 - kT\Lambda$, where Λ is Λ_F with $\tau = \theta_i = 1$. This feature of the configurational Coulomb contribution is generally referred to as a lowering of the ionization potential, and refers to the decrease of the interaction potential between electron and nucleus due to shielding by the surrounding charged particles.

This form of the configurational Coulomb interaction clearly enhances the ionization. Less clear is the fact that it is a minor perturbation that has a relatively small effect and is negligible at high density if it is the only nonideal term considered. Using the free-energy minimization code, a DH Coulomb configurational term was included with an IA model for hydrogen. The resultant equilibrium composition showed slight ionization enhancement, but reached complete recombination at high density. The physical effects responsible for this behavior are first, that when the temperature is low, there are very few charged particles

to interact. When the temperature is high, there are more charged particles, but then the excited states of the atom make a large contribution of the partition function (favoring recombination at higher levels) and also $\Lambda \propto T^{-3/2}$ so that the interaction effect becomes small. Thus, although the Coulomb interactions enhance the ionization, the classical Saha-equation behavior or recombination at high densities is still observed. The interaction term in the free energy vanishes in the limit of infinite volume because $\Lambda \propto V^{-1/2}$ and it vanishes in the limit of zero volume because the plasma recombines into neutral gas particles. Thus, even with the first-order Coulomb effects taken into account, an incorrect equilibrium composition will be calculated if one uses the isolated-atom partition functions. Using a high-order theory for the Coulomb configurational effect increases this incorrect result, as the higher-order terms act to reduce the size of the Coulomb term from its first-order value.

Combining the Coulomb term with the CA model, the resultant equilibrium concentrations are shown in Fig. 5 for the six-component H gas, where total mole number is given for the CA model and the CA model with F_4 as defined in Eq. (5.1). Again the enhancement of ionization is observed at all temperature-volume points where significant ionization exists. The quantitative differences between the two models range from a few percent at 2 eV to 7.5% at 10 eV.

The analytical form for the Coulomb configurational pressure term is

$$P_4 = \frac{F_4}{2V} \left\{ 1 - (3N_e \phi_e / \sum_i N_i z_i^2 \theta_i) - \frac{3}{\tau} \tau - \left(\frac{1}{1+x} \right) \right. \\ \left. \times \left[1 - (N_e \phi_e / \sum_i N_i z_i^2 \theta_i) - \left(2 \frac{\frac{3}{2} kT}{E_F \theta_e} - 1 \right) \right] \right\}, \quad (5.7)$$

where we have assumed that only the electrons need be described by Fermi statistics so that $\theta_i = 1$

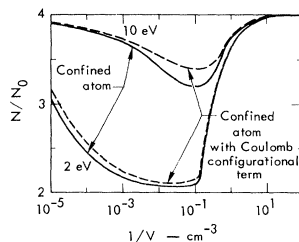


FIG. 5. Equilibrium composition for hydrogen comparing results of the CA model and this model with a modified DH Coulomb configurational term. Increased ionization is present at 2 and 10 eV throughout the intermediate-density region.

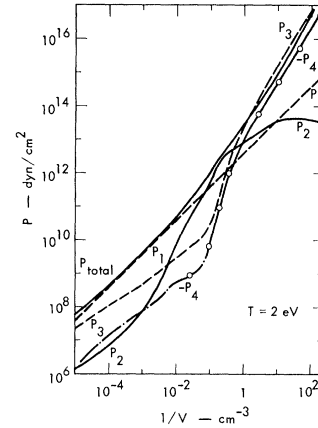


FIG. 6. Equilibrium pressure of hydrogen at 2 eV. The ion pressure P_1 , electron pressure P_3 , and bound-state perturbation P_2 behave very similarly to the CA model (Fig. 4), P_2 remaining the dominant contributor during ionization. The Coulomb pressure P_4 is a negative contributor and its rise parallels that of P_3 , becoming the dominant nonideal term at high density.

for all particles except the electrons (subscript e) and

$$\phi_e = \theta_e - \mathcal{F}_{-3/2}(\alpha_e) / \mathcal{F}_{-1/2}(\alpha_e). \quad (5.8)$$

The quantity ϕ_e approaches zero both for zero degeneracy and for strong degeneracy and is positive otherwise; P_4 is a negative pressure, that is, it represents a pressure contribution of an attractive potential, and tends to "soften" the gas relative to its ideal-gas-pressure values. Note, however, that we have here a contribution which operates in two contradictory directions. The Coulomb interaction operates in the equilibrium calculation to increase the number of particles over the ideal value (hence, if considered by itself, to increase the pressure), but its volume derivative has the opposite sense – it creates a negative pressure due to the attractive potential, and hence, acts to decrease the total pressure. The net effect is smaller total pressure.

The actual pressure values produced by this system are shown in Fig. 6. The Coulomb pressure is negative everywhere, and obtains maximum values that are 32% of the ideal gas pressure at 2 eV, 25% at 5 eV, and 20% at 10 eV. The maximum Coulomb effect occurs as the bound-state perturbations are ionizing the gas, remaining significant at the highest densities shown, where the strongly degenerate translational free energy has become very large. For all temperature values where ionization is significant, the Coulomb interaction must be included to give an accurate physical model of an ionizing gas.

Although the free-energy term used in this analysis is an approximate version of a highly complex physical process, it contains several effects whose individual behavior is important, yet not obvious from the equilibrium results. In Fig. 7, the magnitude of the free energy F_4 has been plotted in three approximations: (i) classical value with Boltzmann statistics and no cutoff; (ii) Fermi statistics used but no cutoff; and (iii) both Fermi statistics and the short-range cutoff included as given by Eq. (5.1).

The classical DH term becomes infinite in the limit of zero volume. This singular behavior demonstrates the invalidity of a first-order plasma theory at high density. The Fermi-modified DH curve shows two characteristics of interest. The first is the uncoupling of the free electrons from the Coulomb interaction as they become degenerate. This is expressed in the θ_i term for electrons since $\theta_e \rightarrow 0$ as $\alpha_e \gg 1$, the limit of large degeneracy. This causes the Fermi-modified DH term to attain lower values relative to the classical term everywhere that electron degeneracy is significant. Since this factor does not affect the ion-ion interaction (until extremely high densities are reached) the modified DH term also reaches very large values as V becomes small. Both these models predict that, at sufficiently high density for any given temperature, the Coulomb pressure P_4 will become larger than the

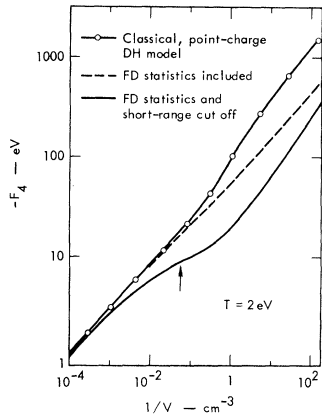


FIG. 7. Coulomb configurational free energy for hydrogen at 2 eV. The classical DH Coulomb term for point charges increases most rapidly with density. The FD-modified DH Coulomb term shows the large decrease in $|F_4|$ produced by including the "uncoupling" of the increasingly degenerate electrons. The short-range cutoff factor leads to even larger decreases in the Coulomb free energy. However, at sufficiently high densities, F_4 increases more rapidly than the $F_1 + F_3$ and the total pressure becomes negative in all these models.

ideal pressure, and being opposite in sign, will produce a negative total pressure. The entire model is invalid long before this point is reached, and here one must turn to the more rigorous quantum cluster expansion theory, which is able to extend the Coulomb model to higher-order terms that are opposite in sign to this first-order term. The next curve in the figure gives F_4^T , the Coulomb term corrected for short-range divergence via the adapted short-range cutoff correction. Here the Coulomb free energy is prevented from becoming too large, as it remains finite and well behaved for all values of V given. However, the arrow marks the point where the $\tau(x)$ correction becomes questionable. A physically more rigorous short-range cutoff is obtained through the action of the uncertainty principle as expressed in the quantum cluster result.⁸ This short-range divergence elimination arises from the many-body theory in a consistent manner and can be extended to the high-order terms.

A quantitative expression for the limit of validity of this model can be given in terms of the degeneracy parameter and the plasma interaction parameter. The model is applicable in the limit of weak degeneracy and weak interactions, given by

$$\alpha_e \leq 0,$$

$$\Lambda_F \leq 0.3.$$

When these limits are exceeded, the more rigorous quantum cluster expansion theory should be used.

6. NON-COULOMBIC INTERACTION EFFECTS

In a real gas, the particles have finite extension, and even for the neutral species, this has an effect on the thermodynamic properties of the gas. As a first approximation to reality, we assume that the particles have a hard core with radius R_i equal to the radius at which the lowest-lying energy level is ionized, as discussed in Sec. 4.

Even for a simple hard-sphere gas, the configurational partition function cannot be obtained exactly for more than a few particles, so it is necessary to make approximations. Let us first make the approximation that the gas is of sufficiently low density that only two-particle collisions are important. We write the configuration integral as

$$\begin{aligned} & \int d\vec{r}_1 \int d\vec{r}_2 \\ & \sim \int d\vec{r}_N \exp[-\beta(u(r_{12}) + u(r_{13}) + \dots)], \end{aligned} \quad (6.1)$$

where the integration of all particle coordinates

is over the volume V . Here, $u(r)$ is the interaction potential between the hard spheres and r_{ij} is the distance between centers of particles i and j . $u(r_{ij})$ is infinite if $r_{ij} < R_i + R_j$ and is zero otherwise. The value of the integrand in (6.1) is therefore unity everywhere except within the collision spheres for particles of type i and j of radius $R_i + R_j$ and volume $\frac{4}{3}\pi(R_i + R_j)^3$, where the integrand is zero. Thus,

$$\int d\vec{r}_{ij} \exp[-\beta u(r_{ij})] = V - \frac{4}{3}\pi(R_i + R_j)^3. \quad (6.2)$$

The complete configurational integral can be evaluated in the approximation that $4\pi N_i(R_i + R_j)^3/(3V) \ll 1$ and its logarithm is given by Fowler,¹¹

$$\sum_i N_i \ln[V - \frac{4}{3}\pi \sum_j N_j 2\pi(R_i + R_j)^3]. \quad (6.3)$$

The finite size of the gas particles, thus, has the effect of adding a term to the free energy of the form

$$F_5 = -kT \sum_i N_i \ln[1 - 2\pi \sum_j N_j (R_i + R_j)^3/3V]. \quad (6.4)$$

It will be noticed that F_5 is always positive and decreases with V . Thus, when the gas is compressed, this term has the effect of increasing the free energy and thus shifting the equilibrium in the direction of smaller numbers of particles having large radii. In particular, it causes pressure ionization. Unfortunately, the validity of this simple theory breaks down at higher densities when the approximation that the ratio of the volume of the particles to the total volume of the gas is much smaller than unity is violated. Clearly, (6.4) breaks down if this ratio is greater than ~ 0.25 .

By adding an excluded volume term such as (6.4) to the IA free energy, a thermodynamically consistent pressure-ionization effect has been achieved, using the free-energy minimization method. The ionization rise at intermediate density is fairly rapid, and the hard-sphere volume reaches the value of 0.25 V at most temperatures. Another disadvantage to using an excluded volume term with the isolated-atom internal partition function is the great discrepancy between the infinite (hard) interparticle potential and the unperturbed internal potential.

By considering the work of adding an additional hard sphere to a mixture, Lebowitz *et al.*¹² have obtained, for the pressure of a hard-sphere mixture, the expression

$$\pi\beta P = 6\xi_0(1 - \xi_3)^{-1} + 18\xi_1\xi_2(1 - \xi_3)^{-2} + 18\xi_2^3(1 - \xi_3)^{-3}, \quad (6.5)$$

$$\text{where } \xi_n = \frac{1}{6}\pi \sum_i (N_i/V)(2R_i)^n. \quad (6.6)$$

They state that this expression gives pressures within a few percent of those produced by machine calculations for binary mixtures with $\xi_3 \lesssim 0.4$. The excess pressure over that of a collection of noninteracting point particles is

$$P_5 = (kT/\pi) [6\xi_0\xi_3(1 - \xi_3)^{-1} + 18\xi_1\xi_2(1 - \xi_3)^{-2} + 18\xi_2^3(1 - \xi_3)^{-3}]. \quad (6.7)$$

Expression (6.7) may be integrated with respect to volume to obtain the part of the Helmholtz free energy due to the finite size of the hard spheres. We find

$$F_5 = (kTV/\pi) [-6\xi_0 \ln(1 - \xi_3) + 18\xi_1\xi_2 \times (1 - \xi_3)^{-1} + 9\xi_2^3(1 - \xi_3)^{-2}]. \quad (6.8)$$

Since from the definition (6.6), ξ_3 is just the ratio of the volume of the hard spheres to the total volume of the gas, $\xi_3 < 1$ and all terms in (6.7) and (6.8) are positive. As V decreases, all the ξ_n increase, F_5 increases and the equilibrium composition is driven toward ionization where most of the particles (nuclei and electrons) have very small radii and contribute less to ξ_1 , ξ_2 , and ξ_3 . A decrease in V increases the pressure in two ways. First, each ξ_n increases as V^{-1} and from (6.7) it can be seen that P_5 increases monotonically with each ξ_n . Secondly, the new equilibrium mixture contains a larger number of particles, and this increases each of the ξ_n also.

The effect of including (6.8) in the free energy is shown for hydrogen in Fig. 8. The effects are negligible at low density, but at higher densities the total number of particles is significantly increased over the case for point particles. This is qualitatively the behavior one would expect in pressure ionization. Note that this is an additional effect to that change in the energy levels of the molecules, atoms, and ions due to interactions.

The equilibrium pressure at 2 eV is illustrated in Fig. 9. The inclusion of the excluded volume term has increased the total gas pressure throughout the intermediate density region by the addition of P_5 , the hard-sphere mixture pressure. This term is the dominant nonideal effect in this region and causes P_2 to become less significant, although still a major term.

The corresponding values of ξ_3 are plotted in Fig. 10 for three temperatures. This demonstrates that $\xi_3 > 0.25$ for most densities at $T \leq 2$ eV, rendering the simple hard-sphere model (6.4) totally invalid here. The hard-sphere

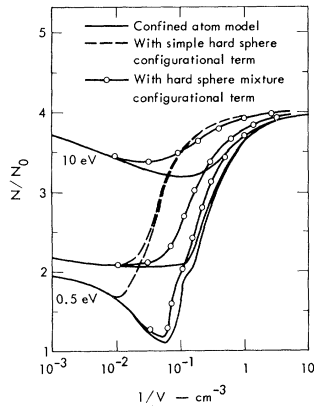


FIG. 8. Equilibrium composition for hydrogen, illustrating the effect of the simple hard-sphere term, and the hard-sphere mixture term compared to the CA model. The simple hard-sphere term is almost temperature-independent for $V^{-1} > 0.2 \text{ cm}^{-3}$, and ξ_3 is everywhere considerably above its limit of 0.25 for applicability of this model. The hard-sphere mixture term produces significant enhancement of ionization and dissociation over the CA model.

mixture model (6.8) is reasonably accurate for all densities at $T \geq 2 \text{ eV}$. This region of validity is extended when a Coulomb term is added to the configurational free energy, which enhances ionization and correspondingly decreases the hard-sphere volume and ξ_3 .

The weak attractive part of the potential between the neutral particles is of importance only

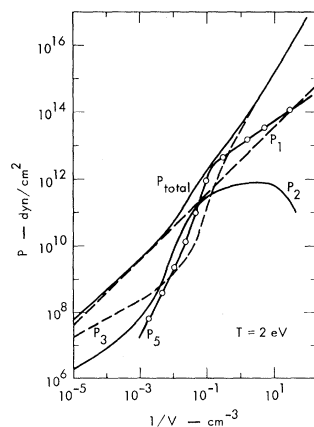


FIG. 9. Equilibrium pressure for hydrogen at 2 eV. Ion pressure (P_1), electron pressure (P_2), and bound-state perturbation pressure (P_3) behave as before. In the intermediate-density region where nonideal effects are a maximum, P_5 , the excluded volume pressure, is the largest contributor, while P_2 is reduced in importance although still an important contributor.

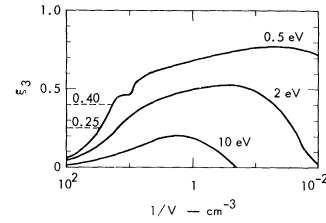


FIG. 10. Excluded volume interaction parameter ξ_3 , as a function of V^{-1} for hydrogen, for the CA model with the hard-sphere mixture configurational free energy. With the simple hard-sphere model ξ_3 would be 10–20% larger at all points. The simple hard-sphere validity limit of $\xi_3 \lesssim 0.25$ is only attained at very high or low volume until $T \gtrsim 10 \text{ eV}$. The hard-sphere mixture limit of accuracy $\xi_3 \lesssim 0.4$ is not exceeded for almost all densities at $T \geq 2 \text{ eV}$.

at relatively low temperatures. The effect of these attractive forces is included in our calculation by means of a van der Waals correction. This correction is for mixtures in the form of a term¹³

$$F_6 = -\sum_i \sum_j x_i x_j a_{ij} / V, \quad (6.9)$$

$$\text{where } a_{ij} = (a_{ii} a_{jj})^{1/2}. \quad (6.10)$$

The a_{ii} are the normal van der Waals constants, and the x_i are the mole numbers of species i .

This correction has the familiar effect on the pressure at low temperatures. The effect on the equilibrium composition is opposite to the pressure-ionization effect, but it is very weak at temperatures where there is an appreciable amount of ionization.

7. EVALUATION OF METHOD

Sections 4–6 have demonstrated the regions where the specific nonideal effects are dominant. Combining these various effects [(4.6), (5.1), and (6.8)] into one complete model yields an improved set of equilibrium thermodynamic properties which incorporate all the nonideal terms. The resultant equilibrium composition and pressure equation of state are given in Figs. 11 and 12. They differ quantitatively from the foregoing results due to the combination of nonideal effects. The number of particles is everywhere as high as or higher than the number obtained by using any of the models of Sec. 4, 5, or 6. The largest differences occur along the 2- and 10-eV isotherms, where F_4 and F_5 both contribute significant perturbations. At 0.5 eV, F_2 and F_5 are the dominant nonideal effects while at 10 eV, F_4 is most important. The pressure

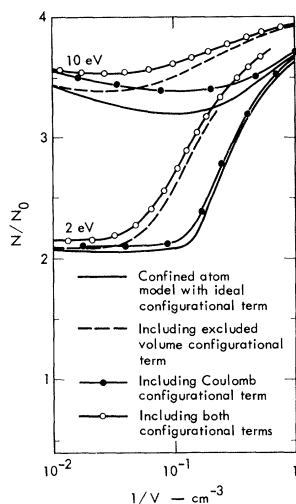


FIG. 11. Comparison of the various nonideal effects on the hydrogen-equilibrium composition. The lowest curves represent the simple CA model (ideal configurational term); the intermediate curves represent the CA model with hard-sphere mixture configurational term only, and with Coulomb configurational term only. The upper curves show the results of the full model with both configurational terms included.

curves show P_2 and P_5 as largest pressure contributors in the intermediate density region at the lower temperatures, while at higher temperatures P_4 becomes large, while P_5 and P_2 become minor contributors. Similar effects are seen in all the thermodynamic properties, the internal energy, specific heats, and compressibility, all demonstrating significant deviation from ideality.

The physical factors which dominate the equilibrium composition calculation are four in number: the classical phase-space factor $VT^{3/2}e^{-\beta E_0}$; the bound-state cutoff $n_{\max}(V, T)$; the bound-state energy-level shift $E_{nl}(V, T)$; and the Coulomb screening effect (lowering of the continuum) represented by Λ_F . The first factor dominates in the classical region at high V and T . The second dominates at high density (low V). The third is important in the intermediate volume region as pressure dissociation and ionization occur, while the Λ factor is also operative in this region. The complex nature of these effects makes it difficult to separate the exact contribution from any one factor at a specific V, T . It is much simpler to use some *ad hoc* criterion based on some physical characteristic of gas particles to obtain uncomplicated formulas for estimating the level cutoff and the ionization equilibrium in various V, T regions. Let us examine how effectively the results of two such simple models compare with the results of this free-energy model.

The first cutoff model, due to Theimer *et al.*¹⁴ suggests that for a high-temperature gas, one can use a cutoff determined by equating the Bohr radius of the highest-bound state with the mean interparticle distance. This criterion leads to an expression for the maximum number of bound states for a hydrogen gas at high temperature,

$$n_{\max}(V) = [a_0^3 \frac{4}{3} \pi (N/V)]^{1/6}.$$

Note that this criterion assumes that n_{\max} depends solely on particle density. With the additional assumptions that $kT \gg E_0$ so that a large number of excited states are important, the internal partition function for the atoms can be reduced to

$$Z_i \approx \frac{2}{3} (n_{\max})^3,$$

and noting that $N_i = N_e$, an equilibrium equation of the following form results:

$$\frac{N(H)}{N(H^+)} \approx \left(\frac{2}{3}\right)^{1/2} \left(\frac{1}{4}\right) \pi e^3 \left(\frac{N}{V}\right)^{1/2} (kT)^{-3/2}.$$

This reduces to

$$\frac{N(H)}{N(H^+)} \approx \left(\frac{1}{64\pi}\right)^{1/2} \Lambda.$$

A simple density dependence criterion for n_{\max} results in a recombination factor linearly proportional to Λ , the plasma parameter (a coincidental result which does not arise from any in-

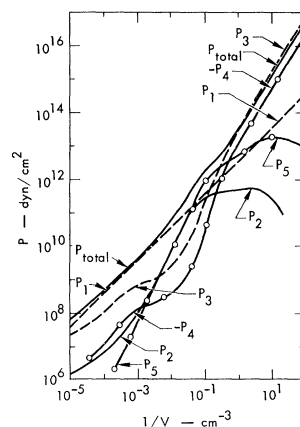


FIG. 12. Equilibrium pressure for hydrogen at 2 eV. The dominant behavior is ideal classical at low density (P_1, P_3), pressure ionization and nonideal effects dominant at intermediate density (P_5 largest, P_2 and P_1 , large), and the degenerate electron gas with strong Coulomb interactions at high density (P_3, P_4).

clusion of plasma terms in the partition function, and in fact predicts the opposite behavior, recombination increasing with Λ).

A second cutoff model, suggested by Riewe and Rompe¹⁵ uses a cutoff criterion which depends only on temperature. Here, the highest bound state is determined by

$$\text{Ryd}/(n_{\text{max}})^2 \leq (kT/T_0),$$

where T_0 is a scale factor. This gives

$$n_{\text{max}}(T) = \left(\frac{2\pi^2 m e^4}{h^2 k (T/T_0)} \right)^{1/2},$$

and with the same assumptions as before

$$N(\text{H})/N(\text{H}^+) \approx T_0^{3/2} \frac{1}{48} \pi^{1/2} \Lambda^2.$$

The temperature-dependent cutoff leads to an equilibrium composition proportional to Λ^2 . The term T_0 may be estimated by using observations of the number of observed hydrogen lines in the solar photosphere, (which yields $T_0 \approx 35$) or by other experimental criteria.

The results obtained for hydrogen with the two simple cutoff models and the FMIN code using the complete CA free-energy model are shown in Fig. 13. The comparison should be limited to

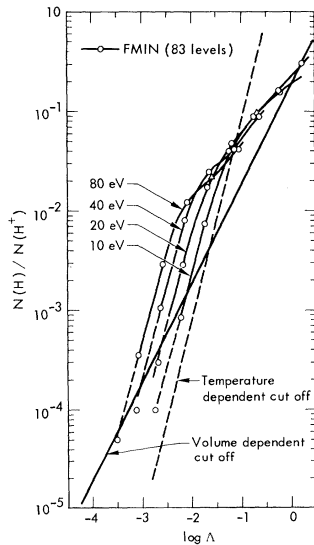


FIG. 13. Hydrogen ionization equilibrium at high temperature, as a function of Λ , the plasma parameter. (The base of the logarithms is 10.) The density-dependent-cutoff model and the temperature-dependent-cutoff model predict equilibria which are functions of Λ only. The complete CA model predicts a more complicated (Λ, T) dependence, which is approximately proportional to Λ^2 in the high- T low- Λ limit.

the high-temperature low-density region, which corresponds to the portion of Λ space where the FMIN ionization curves are linear. The density-dependent (linear Λ) cutoff results do not agree qualitatively with the FMIN compositions, which indicates that this approximation is not well suited for use in high-temperature regions for predicting equilibrium compositions. The temperature-dependent (quadratic Λ) cutoff result has a Λ dependence very similar to the FMIN curves, although it is single valued in Λ space as opposed to the Λ and T dependence of the FMIN results. If T_0 is adjusted, the T -dependent n_{max} would give reasonably accurate composition results over a wide range in V , but a very narrow range in T . The actual high-temperature low-density composition exhibits both V and T dependence. This particular result arises directly from the specific physical model assumed, and only demonstrates that simple cutoff models are probably not sufficient.

In closing, a brief remark on the basic problems and limitations of the free-energy minimization method are in order. The underlying premise of this approach is the factorizability of the total partition function. This becomes increasingly difficult as the density of the system increases and temperature decreases. In the high-density high-temperature limit where a dense-plasma final state is approached, there are theoretical arguments supporting this independence even in the case of the quantum-mechanical many-body partition function.⁹ In the high-density low-temperature limit where a metallic state is approached, the present model does not represent the state of the system accurately. To reach this state, an atomic system with periodic boundary conditions must be included.

A second limitation of the current model is the inaccuracy of our nonhydrogenic eigenstate representations. In principle, the Schrödinger equation for each bound species would contain a potential which exactly reflected the perturbations of the surrounding neutral and charged particles. This potential then would be used in a wave equation for each species to be solved using self-consistent field methods to solve the multi-electron (or multiatom) wave equations, whose results then are used to construct an internal partition function. This is then used in the free-energy model, whose resultant interparticle interaction must agree with the original perturbation potential. This combination of a self-consistent atomic-molecular set of Schrödinger equations with the thermodynamically consistent, free-energy model should produce a reasonably accurate high-density gas theory.

Current modifications of the model include the use of exact numerical solutions of a static screened Coulomb potential for confined one-

electron systems to produce both plasma and neutral atom bound-state perturbations. Both confined atom and periodic boundary conditions are included. This internal model is combined with a configuration term containing a high-order version of the quantum-mechanical cluster expansion theory for dense plasmas.

ACKNOWLEDGMENTS

The authors would like to acknowledge the use of the original free-energy model program to initiate this study, provided by Dr. Gilda M. Harris; and also valuable discussions with Professor Zevi V. Salsburg and Dr. H. E. DeWitt.

*Work performed under the auspices of the U.S. Atomic Energy Commission.

¹G. M. Harris, *J. Chem. Phys.* **31**, 1211 (1959).

²G. M. Harris, J. Trulio, and J. Roberts, *Phys. Rev.* **119**, 1832 (1960).

³S. Chandrasekhar, *Phil. Mag.* **11**, 292 (1930).

⁴S. G. Brush, in *Progress In High Temperature Physics and Chemistry*, edited by C. A. Rouse (Pergamon Press, Inc., London, 1967), Vol. I.

⁵S. R. De Groot and C. A. ten Seldam, *Physics* **12**, 669 (1946).

⁶G. M. Harris, *Phys. Rev.* **124**, 1131 (1962).

⁷F. Herman and S. Skillman, *Atomic Structure Calculations* (Prentice-Hall, Inc., Englewood Cliffs, N.J., 1963).

⁸H. E. DeWitt, *J. Nucl. Energy, Part C: Plasma Phys.* **2**, 224 (1961).

⁹H. E. DeWitt, in *Low Luminosity Stars*, edited by S. Kumar (Gordon and Breach, Science Publishers, Inc., London, 1969).

¹⁰H. Eyring, D. Henderson, B. J. Stover, and E. M. Eyring, *Statistical Mechanics and Dynamics* (John Wiley & Sons, Inc., New York, 1964).

¹¹R. H. Fowler, *Statistical Mechanics* (Cambridge University Press, New York, 1936).

¹²J. L. Lebowitz, E. Helfand, and E. Praestgaard, *J. Chem. Phys.* **43**, 774 (1965).

¹³J. O. Hirschfelder, C. F. Curtiss, and R. B. Bird, *Molecule Theory of Gases and Liquids* (John Wiley & Sons, Inc., New York, 1954).

¹⁴O. Theimer and T. Wright, *Phys. Rev.* **180**, 308 (1969).

¹⁵K. H. Riewe and R. Rompe, *Z. Physik* **111**, 79 (1938).

Wave Damping in Plasma due to Scattering by Ion Sound Waves

H. Gratzl*

*Center for Theoretical Physics, Department of Physics and Astronomy,
University of Maryland, College Park, Maryland 20742*

(Received 12 March 1969)

When high-frequency waves in a plasma are scattered by an enhanced spectrum of low-frequency waves, they lose energy if the resulting secondary waves are Landau damped. Such a nonlinear energy loss of longitudinal waves was calculated hydrodynamically by Sturrock. However, the Vlasov equation gives a more intense scattering. Thus, a wide spectrum of ion sound waves prevents a weak two-stream instability of electron plasma waves more easily than according to the hydrodynamic calculation. If the wave vectors of the ion sound waves are shorter than the width of the instability, the scattering of secondary waves becomes decisive: Electron plasma waves diffuse in k space and the nonlinear stabilizing effect is reduced. Also, transverse high-frequency waves are nonlinearly damped, but less so by a relativistic order at least.

I. INTRODUCTION

When high-frequency waves are scattered by low-frequency waves, the resultant secondary waves are likewise of high frequency. But owing

to the shift of the wave vector, they come in resonance with other particles than the primary waves. Thus, they can be damped linearly, while the primary waves are unstable. Because of the nonlinear coupling through scattering, the primary